

IMPACT OF MHD TURBULENCE ON THE IONIC COMPOSITION OF SOLAR AND STELLAR CORONAE

Paul Lomazzi¹, Victor Réville¹, Alexis Rouillard¹, Pascal Petit¹

¹IRAP, Université Toulouse III - Paul Sabatier, CNRS, CNES, Toulouse, France

Spectroscopic observations of the solar atmosphere reveal regions of the solar corona that are enriched in the abundance of heavy element with low-first ionisation potential (examples of low 'FIP' i.e. with <10 eV are Fe, Mg) relative to photospheric abundances¹. This enhancement in the abundance of low-FIP elements by a factor of three or four, called the 'FIP effect', is still not well understood. Moreover enriched abundances of low-FIP elements are also observed in the slow solar wind, which could give us more insights on its origins. An inverse-FIP effect corresponding to a decreased abundance of low-FIP elements has been measured in the atmosphere of M-type stars². Turbulent mixing of the chromosphere combined with the ponderomotive force caused by Alfvén waves propagating in these atmosphere could give a mechanism that might explain both the FIP and inverse FIP effect³. Our goal is to study the role of magnetic topology and turbulence on this fractionation mechanism. In this work we use a MHD code to simulate wind profiles through which Alfvénic perturbations are propagated. We compare simulation outputs from two types of models, full MHD and a Shell model of Alfvén-wave turbulence.

MHD simulation of the Solar Wind Background

A background equilibrium is generated by solving 1D ideal MHD equations. A phenomenological heating is added to generate slow wind. The magnetic field profile is computed through the expansion factor f_{exp} which greatly expand in the corona but does not include a funnel. The background solar wind modeled using our 1-D MHD code is shown in Figure 1.

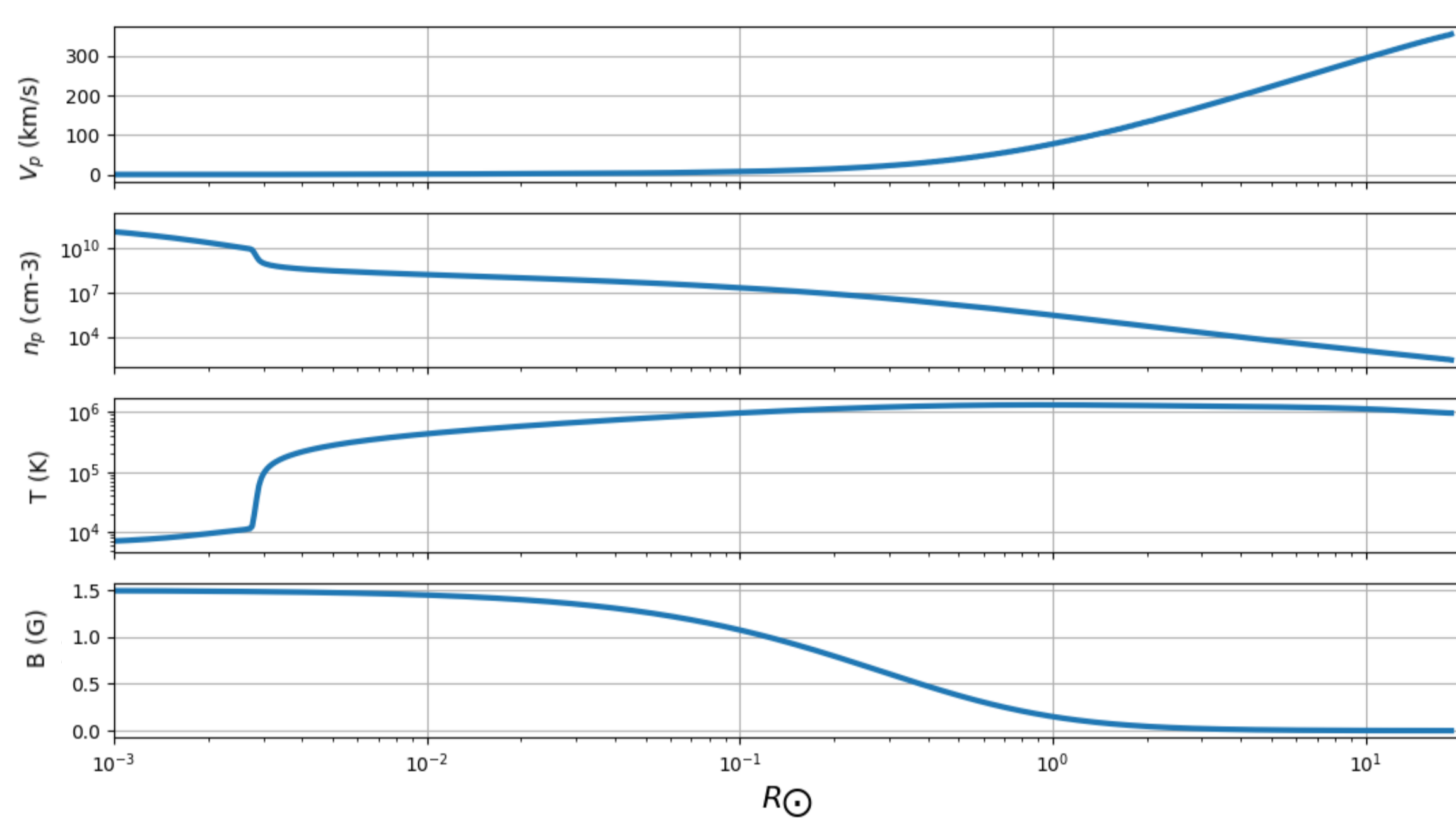


Figure1: Some plasma characteristics profile as a function of radial distance for MHD Sim with solar parameters. From top to bottom : velocity, density, temperature and magnetic field. The density and the temperature respectively strongly decrease and increase at the transition region at 3E-3 solar radii. The pressure gradient accelerates the plasma and generates the solar wind.

Alfvén-wave propagation and its induced ponderomotive acceleration

Torsional Alfvén waves are self-consistently propagated from the bottom of the domain to 20 solar radii through a non uniform media with varying Alfvén speed.

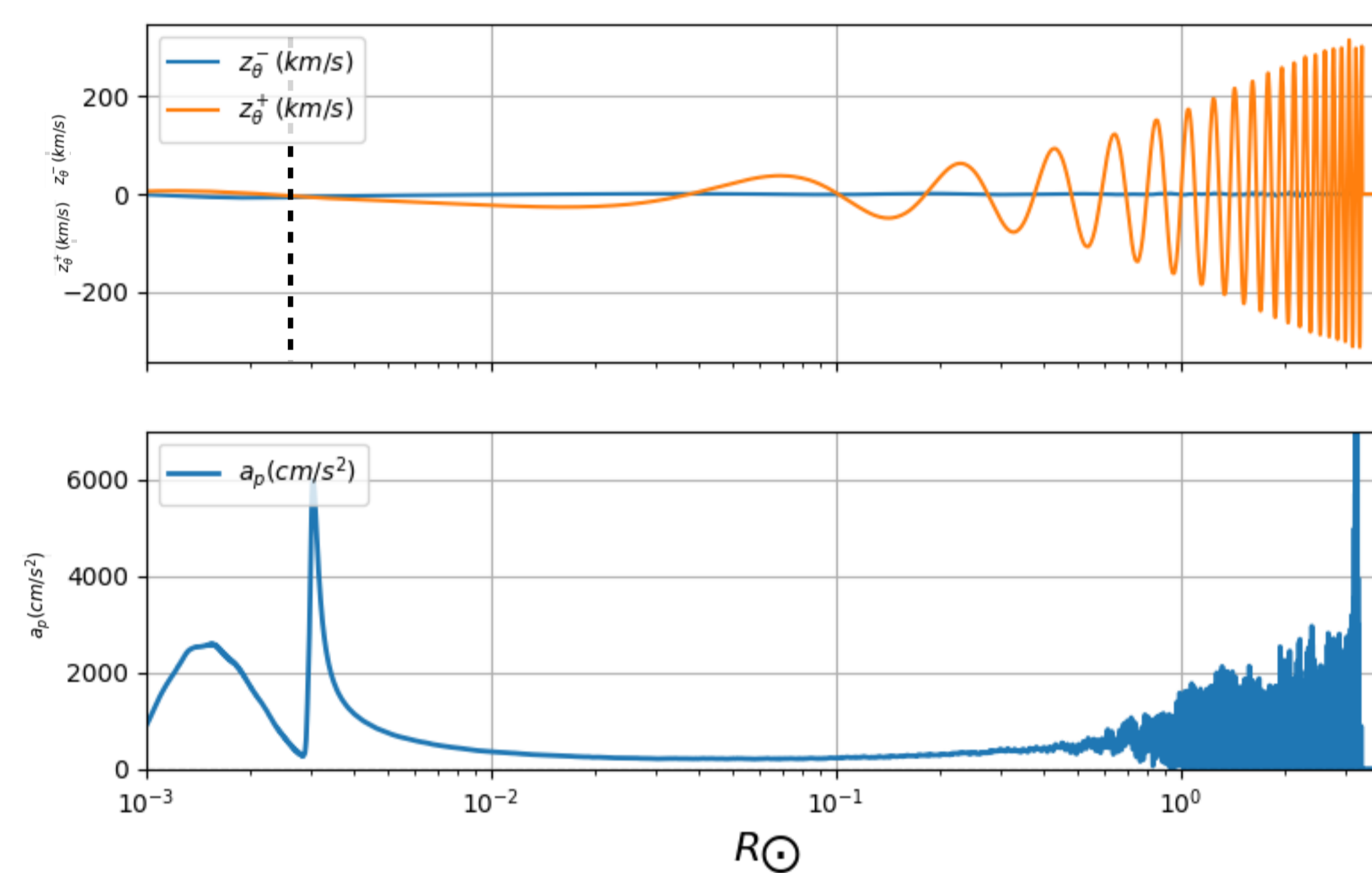


Figure2: Top panel : Elsasser variables showing the downstream and upstream (reflected) waves. The reflection is due to the non uniform Alfvén speed induced by the density and magnetic field non uniformity. The reflected wave (blue) amplitude is the same as the transmitted (orange) one in the chromosphere because of the very steep density gradient at the TR, generating very strong reflection. In the corona, the reflected part of the wave is negligible compared the transmitted part.

$$z^{\pm} = v \pm \frac{B}{\sqrt{\mu\rho}}$$

A ponderomotive force naturally arises when a wave propagates in a non uniform plasma through the gradient of the squared electric field strength, E . It is a non linear force acting as a wave pressure on charged particles in the direction of the gradient of the E field.

The ponderomotive acceleration induced by low-frequency waves, (i.e. waves with frequency much less than the ion gyrofrequency) is given by ³:

$$a_{w,s} = \frac{\partial}{\partial s} \left[\frac{\langle \delta E^2 \rangle}{2|B|^2} \right] \quad (1)$$

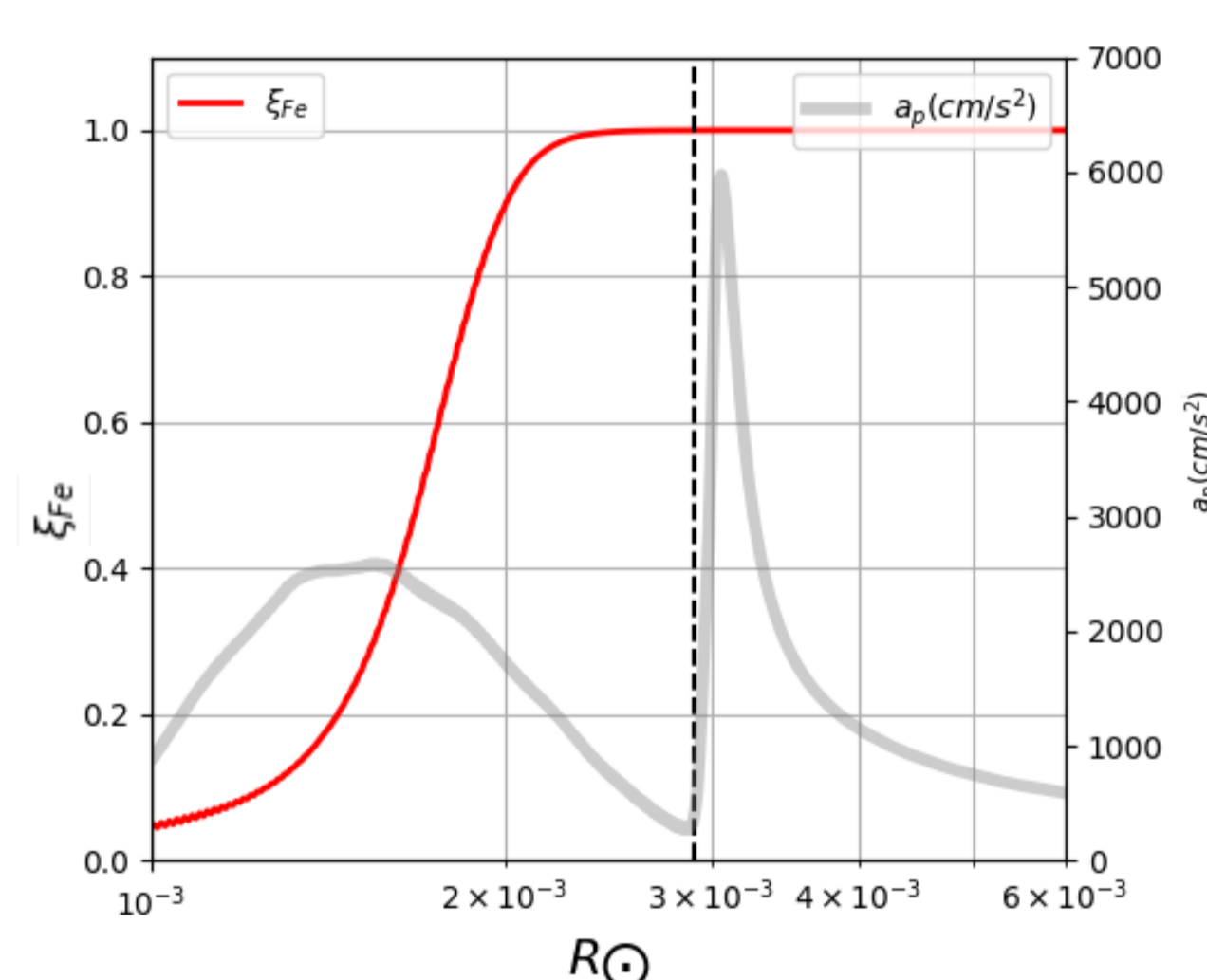
The ponderomotive acceleration is independent of the ion mass as suggested by spectroscopic observations of the solar corona and solar wind data.

Saturation effects of the ponderomotive force can be induced by instabilities and wave-mode conversion such as the generation by Alfvén waves of acoustic waves.

Simulation results : FIP bias

In this first application we use Saha equation to determine the ionisation fraction profile of different elements through the chromosphere.

Figure3: Ionisation profile (red) of iron which is a low FIP element. It begins to ionise inside the region of high ponderomotive acceleration giving rise to a important FIP bias as stated by equation (2). Elements with high FIP will ionise near the TR inducing a weaker FIP bias.



We compute the FIP bias for three low FIP elements (Mg, Fe, Si) and one high FIP element (O) with $v_T=4\text{km/s}$

| | FIP Bias (Sim) | FIP bias (Obs) ⁴ |
|----|----------------|-----------------------------|
| Mg | 3.07 | 4±0.3 |
| Fe | 3.02 | 5±2 |
| Si | 2.07 | 4.5±0.5 |
| O | 1.52 | 1±0.1 |

The FIP bias between the photosphere and the corona is then computed using³ :

$$\frac{\rho_j^{\text{cor}}}{\rho_j^{\text{chr}}} = \exp\left(\int_{z_{\text{chr}}}^{z_{\text{cor}}} \frac{\xi_j a_{w,s} v_{\text{eff}}}{\gamma_{ji} v_j^2} dz\right) \quad (2)$$

$$v_j^2 = c_{sj}^2 + v_T^2$$

The FIP bias is very dependent on the choice of the turbulent mixing velocity, v_T , limiting mass-dependent induced by gravitational settling.

Shell ATM results⁵

We then self-consistently propagate perturbations using a 1-D shell turbulence model. This time, the wave is non monochromatic as multiple wavelength are excited at the start, which will generate a turbulent cascade. In contrast to the previous full MHD approach, compressive modes are not taken into account in this model. We use the same background parameters as the previous MHD simulation.

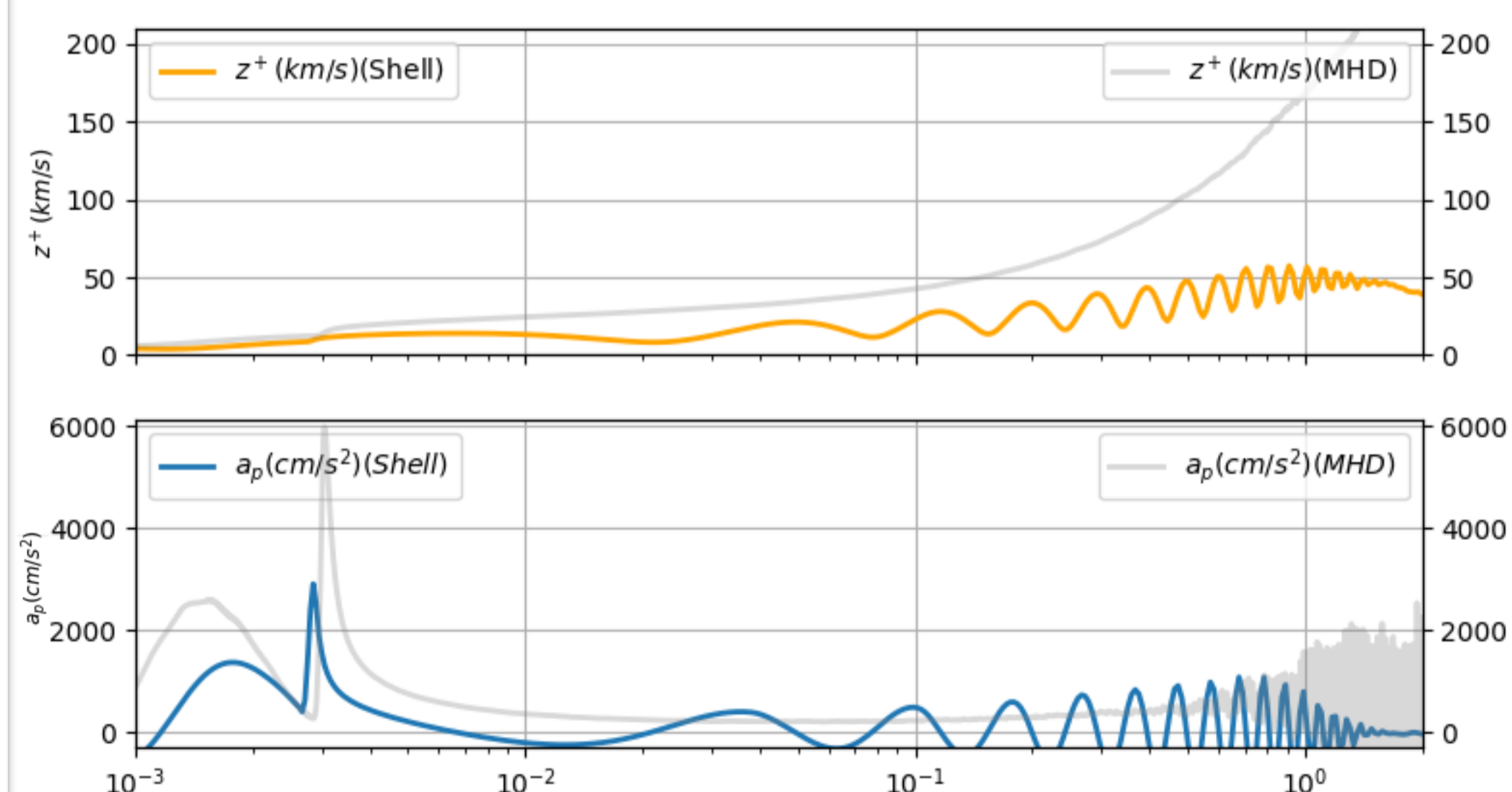


Figure4: Top panel : Amplitudes of elsasser variables showing the jump at the transition region.

Bottom panel : Ponderomotive acceleration calculated with (1). The spike and bump are still there but the amplitude is reduced by a factor of 2. There are strong oscillations in the corona which can't be due to a parametric instability.

In this simulation, a weaker ponderomotive acceleration results in a lower FIP bias.

| | FIP Bias (Sim) |
|----|----------------|
| Mg | 1.88 |
| Fe | 1.75 |
| Si | 1.43 |
| O | 1.22 |

Future work will include:

- Varying parameters to get closer to M stars conditions (Higher magnetic field, higher density, lower temperature).
- Testing J.M. Laming's theory for inverse FIP effect using 2D MHD simulations to get realistic mode conversions
- Using a 1D kinetic fluid model developed at IRAP we will also account for the collisional effects of heavy ions moving through the proton-dominated plasma.

¹Feldman, U. (1992). Elemental abundances in the upper solar atmosphere.

²Wood, B. E., & Linsky, J. L. (2010). Resolving the ξ Boo binary with Chandra, and revealing the spectral type dependence of the coronal "FIP effect."

³Laming, J.M. (2015). The FIP and Inverse FIP Effects in Solar and Stellar Coronae.

⁴Geiss, Johannes. (1998) Constraints on the FIP Mechanisms from Solar Wind Abundance Data.

⁵Buchlin, É., & Velli, M. (2006). Shell Models of RMHD Turbulence and the Heating of Solar Coronal Loops.